Anomalous dynamics in multilevel quantum decay

Stefano Longhi
Dipartimento di Fisica, Politecnico di Milano and Istituto di Fotonica e Nanotecnologie del Consiglio Nazionale delle Ricerche, Piazza L. da Vinci 32, I-20133 Milano, Italy

(Received 24 July 2018; published 27 August 2018)

A metastable quantum state coupled to a continuum undergoes an exponential decay in the Weisskopf-Wigner (Markovian) approximation. However, quantum theory strictly predicts deviations from an exponential decay law both at small and long time scales. In multilevel systems, even in the Markovian approximation strong deviations from an exponential decay can be observed in the intermediate time scale owing to interference of overlapping resonances. Such interference effects are simply described by an effective non-Hermitian Hamiltonian and are known to explain, for example, the existence of dark states and fractional decay. Here we show that the wide variety of anomalous behaviors observed in multilevel quantum decay are rooted in the non-normal nature of the effective non-Hermitian Hamiltonian, revealing strong similarities between anomalous quantum mechanical decay and non-normal dynamics found in hydrodynamic flows. Major signatures of non-normal dynamics include delayed decay, accelerated decay, and exponential-power-law decay at an exceptional point. Such signatures are exemplified by suggesting simple tight-binding lattice realizations of multilevel quantum decay, which could be emulated in integrated photonic experiments. Finally, it is shown that for noninteracting particles with fermionic statistics the usual exponential decay law is restored, i.e., all anomalous decay effects arising from single-particle non-normal dynamics are washed out.

DOI: 10.1103/PhysRevA.98.022134

I. INTRODUCTION

Decay of an unstable quantum state into a continuum is a fundamental physical process which has received great theoretical interest since the early developments of quantum mechanics [1–8]. Quantum decay is ubiquitous in a wide variety of physical systems involving unstable elementary particles, nuclei, atoms, and molecules. Examples include the nuclear alpha decay [1], spontaneous emission of a photon from an atomic excited state [2], atomic autoionization [5], tunneling escape from a potential trap [3], etc. In the Weisskopf-Wigner (Markovian) approximation [2], an exponential law is known to well describe quantum mechanical decay. However, exact quantum mechanical calculations predict that the survival probability is definitely not exponential at short and long times (see, e.g., Refs. [4–12] and references therein). Such deviations have been clearly observed in some recent experiments [13,14]. Major consequences of nonexponential decay at short times are Zeno and anti-Zeno effects, i.e., deceleration or acceleration of the quantum decay by frequent or infrequent measurements (see, e.g., Refs. [15–20] and references therein). In many-body systems, the decay dynamics can be modified by particle statistics and contact interactions [21,22]. Quantum decay is further modified when two or more metastable states decay into a common continuum. Long-time behavior of the decay dynamics in multilevel quantum systems has been studied, for example, in Ref. [23]. Major features in multilevel quantum decay are related to the appearance of quantum interference among different resonances of the system. Such features can be captured rather generally within the Markovian approximation. Under certain conditions, perfect destructive interference of different decay channels can arise, resulting in a limited decay and the existence of bound states in the continuum (also referred to as dark states) [24,25]. However, it is generally impossible to satisfy the destructive interference conditions simultaneously for all the transitions when many metastable states are involved, i.e., limited decay is observed in very special cases. Nonetheless, interference of resonance states generally results in appreciable deviations from an exponential decay in the intermediate time scale, even when the Markovian approximation is used. Such deviations include damped oscillations [26], resilient periods followed by decay bursts [27], and exponential-power-law decay near an exceptional point (EP) [28].

In this work it is shown that the wide variety of anomalous decay behaviors observed in multilevel quantum decay are rooted in the non-normal nature of the effective non-Hermitian Hamiltonian that describes interference of the resonance states, thus sharing a strict connection with the non-normal dynamical behavior observed in hydrodynamic flows [29,30]. Major signatures of non-normal dynamics include delayed decay, accelerated decay, and exponential-power-law decay at an exceptional point. Such effects are here exemplified by suggesting simple tight-binding lattice realizations of multilevel quantum decay, which could be emulated using photonic waveguide lattices [31]. Finally, we briefly discuss multiparticle quantum decay and show that for noninteracting fermionic particles all anomalous decay effects arising from non-normal dynamics can be washed out and an exact single exponential decay law is restored.

II. MULTILEVEL QUANTUM DECAY: BASIC EQUATIONS AND EFFECTIVE NON-HERMITIAN MODEL

A rather general framework to study multilevel quantum decay is provided the Friedrichs-Lee (or Fano-Anderson) model,

which describes the decay of N discrete states coupled to one (or more) continuum of states. For the sake of definiteness, we will focus our analysis to the case where the N discrete states are coupled to a common continuum of states; however, a similar study could be extended *mutatis mutandis* to the case where more than one continuum is involved in the decay dynamics (see Sec. III C for an example involving more than one continuum). The second-quantization Hamiltonian of the N-level Friedrichs-Lee model reads

$$\hat{H} = \sum_{n=1}^{N} \omega_n \hat{c}_n^\dagger \hat{c}_n + \int dk\, \omega(k) \hat{c}^\dagger(k) \hat{c}(k) + \sum_{n=1}^{N} \int dk [g_n(k) \hat{c}_n^\dagger \hat{c}(k) + g_n^*(k) \hat{c}^\dagger(k) \hat{c}_n]. \quad (1)$$

In the above equation, $\hat{c}_n$, $\hat{c}_n^\dagger$ are the annihilation and creation operators of particles for the bound states at energies ω_n ($n = 1, 2, \ldots, N$), $\hat{c}(k)$, $\hat{c}^\dagger(k)$ are the annihilation and creation operators of particles in the continuum states at the energy $\omega(k)$, and $g_n(k)$ is the spectral coupling function between the nth discrete level and the continuum. The operators $\hat{c}_n$, $\hat{c}_n^\dagger$, $\hat{c}(k)$, $\hat{c}^\dagger(k)$ satisfy the usual commutation or anticommutation relations of bosonic or fermionic particles. The Hamiltonian $\hat{H}$ commutes with the particle number operator $\hat{G} = \sum_n \hat{c}_n^\dagger \hat{c}_n + \int dk\, \hat{c}^\dagger(k) \hat{c}(k)$, which is thus a constant of motion. In the single-particle case $G = 1$, particle statistics is not of relevance and the state vector of the system can be expanded as

$$|\psi(t)\rangle = \sum_{n=1}^{N} c_n(t) \hat{c}_n^\dagger |0\rangle + \int dk\, c(k,t) \hat{c}^\dagger(k) |0\rangle, \quad (2)$$

where $c_n(t)$ and $c(k,t)$ are the probability amplitudes to find the particle at the nth discrete level or in the continuum, respectively, with the normalization condition $\sum_n |c_n(t)|^2 + \int dk |c(k,t)|^2 = 1$. Assuming $\hbar = 1$, the evolution of the amplitude probabilities is governed by the coupled equations

$$i \frac{dc_n(t)}{dt} = \omega_n c_n + \int dk\, g_n(k) c(k,t), \quad (3)$$

$$i \frac{\partial c(k,t)}{\partial t} = \omega(k) c(k,t) + \sum_{n=1}^{N} g_n^*(k) c_n(t). \quad (4)$$

The degrees of freedom of the continuum can be formally eliminated from Eqs. (3) and (4), yielding the following integro-differential equations for the occupation amplitudes c_n of the discrete states

$$i \frac{dc_n}{dt} = \omega_n c_n - i \sum_{m=1}^{N} \int_0^t d\xi\, \mathcal{G}_{n,m}(t-\xi) \times \exp[-i\omega_m (t-\xi)] c_m(\xi), \quad (5)$$

where we have set

$$\mathcal{G}_{n,m}(\tau) \equiv \int dk\, g_n(k) g_m^*(k) \exp\{i[\omega_m - \omega(k)]\tau\} \quad (6)$$

and assumed $c(k,0) = 0$. The Weisskopf-Wigner (Markovian) approximation is introduced as usual by considering the weak-coupling limit $g_n \to 0$ and assuming a nonstructured continuum. This yields an effective non-Hermitian dynamics for the evolution of the amplitude probabilities $c_n(t)$, which reads

$$i \frac{dc_n}{dt} = \sum_m \mathcal{H}_{n,m} c_m(t), \quad (7)$$

where the elements of the $N \times N$ non-Hermitian matrix $\mathcal{H}$ are given by

$$\mathcal{H}_{n,m} = \omega_n \delta_{n,m} - i \Delta_{n,m} \quad (8)$$

and where we have set

$$\Delta_{n,m} \equiv \int_0^\infty d\tau\, \mathcal{G}_{n,m}(\tau) = \int_0^\infty d\tau \int dk\, g_n(k) g_m^*(k) \exp\{i[\omega_m - \omega(k)]\tau\}. \quad (9)$$

The survival probability, i.e., the probability that the particle has not decayed into the continuum at time t, is given by

$$P(t) = \sum_{n=1}^{N} |c_n(t)|^2, \quad (10)$$

with $P(0) = 1$ and $P(t) \leqslant 1$ for any $t \geqslant 0$. In the following, we will assume that the frequencies ω_n of discrete levels are embedded in the continuous spectrum of scattering states and that there are not bound states in the continuum, i.e., $P(t) \to 0$ as $t \to \infty$.

III. NON-NORMAL DECAY DYNAMICS

A. General aspects

In the Markovian approximation, the decay dynamics $P(t)$ is determined by the properties of the non-Hermitian matrix $\mathcal{H}$. At first sight one could think that the decay dynamics is essentially established by the energy spectrum, i.e., eigenvalues of $\mathcal{H}$, and that the eigenvalue with the largest imaginary part (i.e., minimum decay rate) gives the dominant term of the decay dynamics of $P(t)$. This picture is rather satisfactory in many cases, for example, to describe limited decay when there exist bound states in the continuum, signaled by the existence of one (or more) eigenvalues of $\mathcal{H}$ with vanishing imaginary part, or whenever $\mathcal{H}$ is a normal operator. However, it can fail to describe important dynamical effects when $\mathcal{H}$ is non-normal, i.e., when the commutation relation

$$\mathcal{H}^\dagger \mathcal{H} = \mathcal{H} \mathcal{H}^\dagger \quad (11)$$

is not satisfied. For non-normal operators, i.e., when $\mathcal{H}^\dagger \mathcal{H} \neq \mathcal{H} \mathcal{H}^\dagger$, the energy spectrum of $\mathcal{H}$ and the spectral dominance established by the long-lived resonance mode may have little to do with the dynamical behavior of the system [29,30]. This somewhat unusual behavior is observed, for example, in hydrodynamics flows, where turbulence can arise in spite of eigenvalue stability of the underlying flow [29]. In the following, we will assume that there are not dark states, and that $P(t)$ undergoes a complete decay. Let us indicate by $\lambda_1, \lambda_2, \ldots, \lambda_N$ the eigenvalues of $\mathcal{H}$, ordered such that $0 < \mathrm{Im}(\lambda_1) \leqslant \mathrm{Im}(\lambda_2) \leqslant \cdots \leqslant \mathrm{Im}(\lambda_N)$, and let us set

$$P(t) = F(t) \exp(-t/\tau), \quad (12)$$

where

$$\frac{1}{\tau} \equiv 2|\mathrm{Im}(\lambda_1)|. \tag{13}$$

Note that τ is the lifetime of the long-lived resonance mode of the decaying system. Deviations of the decay law $P(t)$ from the exponential decay of the long-lived resonance mode are embedded in the function $F(t)$. The following general properties of $F(t)$ and $P(t)$ can be readily proven (see Appendixes A and B for some technical details).

(i) The upper and lower bounds for $P(t)$, when the initial condition $\mathbf{c}(0) \equiv (c_1(0), c_2(0), \ldots, c_N(0))^T$ is varied, are given by

$$\sigma_{\min}(t) \leqslant P(t) \leqslant \sigma_{\max}(t), \tag{14}$$

where $\sigma_{\min}(t)$ and $\sigma_{\max}(t)$ are the smallest and largest eigenvalues of the matrix $\mathcal{A}^\dagger\mathcal{A}$ and where we have set $\mathcal{A} \equiv \exp(-i\mathcal{H}t)$. The largest (smallest) value $\sigma_{\max}$ ($\sigma_{\min}$) is assumed for the initial excitation $\mathbf{c}(0)$ of the system which is the eigenvector of $\mathcal{A}^\dagger\mathcal{A}$ with eigenvalue $\sigma_{\max}$ ($\sigma_{\min}$).

(ii) If the non-Hermitian matrix $\mathcal{H}$ is normal, i.e., if $\mathcal{H}$ satisfies the commutation relation (11), then

$$\sigma_{\max}(t)=\exp(-t/\tau), \quad \sigma_{\min}(t)=\exp(-2t|\mathrm{Im}(\lambda_N)|). \tag{15}$$

In other words, for a normal matrix $\mathcal{H}$ the decay cannot be slower than the long-lived resonance mode nor faster than the less-lived resonance mode of the system. In particular, this means that $F(t) \leqslant 1$, and $F(t) = 1$ if and only if the initial state $\mathbf{c}(0) \equiv (c_1(0), c_2(0), \ldots, c_N(0))^T$ of the system is the eigenvector of $\mathcal{H}$ corresponding to the eigenvalue λ_1.

(iii) Let us assume that $\mathcal{H}$ is a defective matrix and that the eigenvalue λ_1 is an EP of $\mathcal{H}$ of order h, with $2 \leqslant h \leqslant N$. This means that h eigenvalues and corresponding eigenvectors of $\mathcal{H}$ coalesce [32,33]. Indicating by $\mathbf{v}_1$ the eigenvector of $\mathcal{H}$ with eigenvalue λ_1 and by $\mathbf{u}_2, \mathbf{u}_3, \ldots, \mathbf{u}_h$ the chain of associated (generalized) eigenvectors (see Appendix B for the definition of associated eigenvectors of a defective matrix), in the asymptotic limit $t \to \infty$ one has

$$F(t) \simeq \frac{(\mathbf{v}_1|\mathbf{v}_1)}{[(h-1)!]^2(\mathbf{u}_h|\mathbf{u}_h)} t^{2(h-1)}, \tag{16}$$

where $(\mathbf{f}|\mathbf{g}) \equiv \sum_n g_n^* f_n$ denotes the usual l^2 scalar product. Moreover, the initial system excitation $\mathbf{c}(0)$ that realizes the largest survival probability in the $t \to \infty$ asymptotic limit is the generalized eigenvector $\mathbf{u}_N$.

The above properties highlight the major impact that the non-normal nature of $\mathcal{H}$ plays in the appearance of anomalous decay behaviors. In fact, owing to property (ii), in a decaying multilevel system described by a normal Hamiltonian $\mathcal{H}$ effects such as transient initial resilient (nondecaying) behavior or power-exponential decay in the intermediate or long time scales are prevented. Such effects could be of major interest in quantum decay control contexts; for example, initial nondecaying dynamics could be exploited to slow down quantum decay by infrequent interruptions, i.e., by kicking the system at time intervals much longer than the characteristic Zeno time [26].

Here we illustrate two non-normal decay behaviors in a multilevel system occurring at short and intermediate or long time scales, suggesting simple tight-binding lattice realizations of the proposed models.

B. Delayed and accelerated decay

An interesting behavior of a non-normal Hamiltonian $\mathcal{H}$ is to allow for delayed and accelerated decays arising from quantum interference of decaying resonance modes. Such effects are very different than well-established Zeno or anti-Zeno effects, i.e., the deceleration or acceleration of quantum decay by frequent observations of the system below or above the Zeno time [15–19], and received little attention so far.

Delayed decay occurs when $\sigma_{\max}(t)$ remains very close to one for some interval $0 < t < \tau_d$, after which the decay starts, usually with an abrupt drop of $P(t)$. Such a resilient behavior, with the decay effectively starting after the delay time τ_d, was earlier noticed in Ref. [27] in the case of two and three interference resonances in an atom interacting with the quantum vacuum of electromagnetic field, suggesting a way to slow down spontaneous emission decay. Clearly, delayed decay is a signature of non-normal dynamics since it is forbidden for a normal Hamiltonian $\mathcal{H}$ [according to property (ii) stated in Sec. III A]. Here we present an example of a decaying multilevel system showing a resilient time τ_d that can be made arbitrarily long as the number N of interfering resonances is increased, suggesting a very simple realization of the model based on hopping dynamics in a tight-binding lattice. This model also provides a very simple and intuitive explanation of the delayed decay behavior, and could be emulated in photonic waveguide lattices. Likewise, we show that accelerated decay as a result of non-normal dynamics is possible in such a model for a different initial preparation of the system. This means that, by changing coherent initial excitation of the N levels, the decay dynamics can be either slowed down or accelerated as compared to the lifetimes of the long-lived and less-long-lived resonance states of the system.

Let us specialize the Friedrichs-Lee Hamitonian (1) by assuming the following form of energies ω_n, $\omega(k)$ and spectral coupling functions $g_n(k)$:

$$\omega_n = 2\kappa \cos\left(\frac{n\pi}{N+1}\right), \tag{17}$$

$$\omega(k) = 2\Delta \cos k, \tag{18}$$

$$g_n(k) = \frac{\rho}{\sqrt{\pi(N+1)}} \sin\left(\frac{n\pi}{N+1}\right), \tag{19}$$

where $n = 1, 2, \ldots, N$, $-\pi \leqslant k < \pi$, and κ, Δ, and ρ are some positive constants. Clearly, the continuum of scattered states, into which the N discrete levels decay, is a tight-binding continuum with a bandwidth 4Δ, and the discrete levels are homogeneously coupled to the continuum, i.e., the spectral coupling functions g_n are independent of k. The model (17)–(19) has a very simple physical realization, which is illustrated in Fig. 1 and discussed in details below. After some lengthy but straightforward calculations, the coefficients $\Delta_{n,m}$ entering in the non-Hermitian matrix $\mathcal{H}$ [Eqs. (8) and (9)] can be calculated

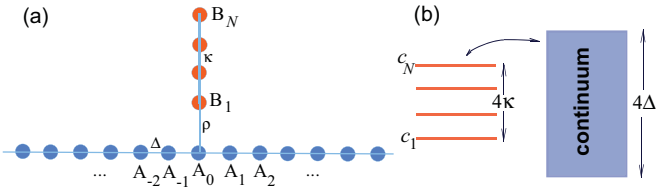

FIG. 1. (a) Tight-binding model of multilevel quantum decay showing non-normal anomalous decay. The system comprises a chain of N discrete Wannier states $|n\rangle$, $n = 1, 2, \ldots, N$, for example a quantum dots chain, attached to a tight-binding array (a quantum wire) that provides the continuum of states where the discrete levels decay. Δ and κ are the hopping rates between adjacent sites in the lattice and in the chain, respectively, whereas $\rho < \Delta$ is the chain-lattice coupling. A_n ($n = 0, \pm 1, \pm 2, \ldots$) and B_n ($n = 1, 2, \ldots, N$) are the occupation amplitudes of sites in the quantum wire and in the quantum dots chain, respectively. (b) Schematic of the energy levels of the corresponding Friedrichs-Lee Hamiltonian in the Bloch basis.

in a closed form and read

$$\Delta_{n,m} = \frac{\rho^2}{\Delta(N+1)} \frac{1}{\sqrt{1-\left(\frac{\omega_m}{2\Delta}\right)^2}} \times \sin\left(\frac{n\pi}{N+1}\right) \sin\left(\frac{m\pi}{N+1}\right). \tag{20}$$

Figure 2 shows a typical behavior of the boundaries $\sigma_{\min}(t)$ and $\sigma_{\max}(t)$ of the survival probability $P(t)$, and corresponding exponential decay of long-lived and less-long-lived resonance modes of the system, for a few increasing values of number N of discrete states. Note that $\sigma_{\max}(t)$ remains very close to one for a resilient time τ_d, after which a rather abrupt drop is observed, corresponding to a delayed decay [see lower panels in Figs. 2(a)–2(c)]. Interestingly, the resilient time τ_d is an increasing function of the number N of discrete levels, as shown in Fig. 2(d). Conversely, the behavior of $\sigma_{\min}(t)$ shows an abrupt drop in the initial stage of decay, well below the less-long-lived resonance of the system, indicating that the decay can be accelerated by a suitable initial coherent preparation of the discrete states. Figure 3(a) shows an example of the numerically computed behavior of the survival probability $P(t)$ for two different initial preparations of the system, corresponding to the eigenvectors of $\mathcal{A}^\dagger\mathcal{A}$ (calculated at the time $t = t_0 \sim \tau_d$) with largest and smallest eigenvalues [see Figs. 3(b) and 3(c)]. Solid and dashed curves, almost overlapped, refer to the numerical results obtained with and without the Markovian approximation. The plots clearly show delayed and accelerated decay dynamics, and demonstrate the accuracy provided by the Markovian approximation.

The Friedrichs-Lee Hamiltonian with frequencies and spectral couplings defined by Eqs. (17)–(19) has a very simple physical implementation, based on particle hopping in a tight-binding lattice as illustrated in Fig. 1(a). The system comprises a chain of N Wannier sites (such as a chain of quantum dots) with hopping amplitude κ, which is attached via a hopping constant ρ to a one-dimensional infinite tight-binding lattice (i.e., a quantum wire) with hopping rate Δ. The quantum wire provides the tight-binding continuum of scattering states where excitation is in the chain decay. This system can be

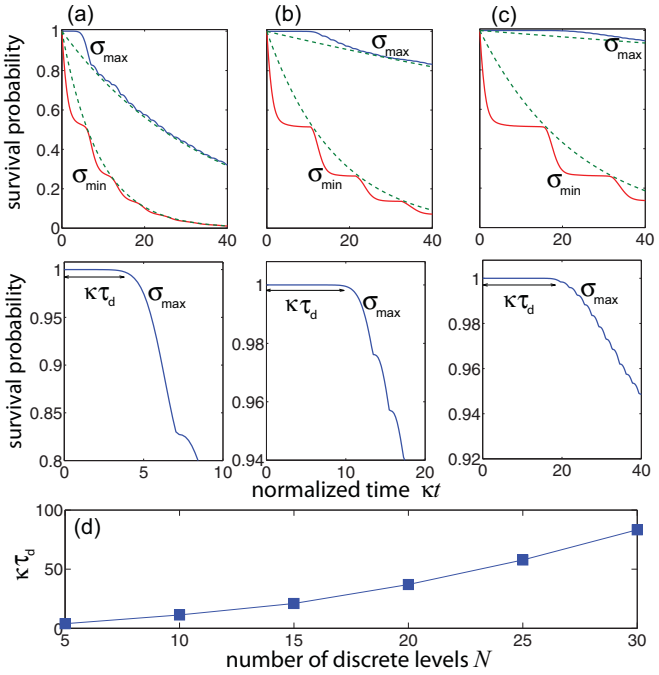

FIG. 2. (a)–(c) Numerically computed behaviors of the upper ($\sigma_{\max}$) and lower ($\sigma_{\min}$) boundaries of the survival probability $P(t)$ versus normalized time for the tight-binding lattice model of Fig. 1(a) and for parameter values $\rho/\kappa = 1$ and $\Delta/\kappa = 3$. The number N of discrete levels is $N = 5$ in (a), $N = 10$ in (b), and $N = 15$ in (c). The dashed lines correspond to the exponential decay behaviors of long-lived (eigenvalue λ_1) and less-long-lived (eigenvalue λ_N) resonances of the decaying levels. The lower panels in (a)–(c) show an enlargement of the upper boundary $\sigma_{\max}$ in the early stage of the decay, clearly demonstrating resilient dynamics and delayed decay. Panel (d) shows the numerically computed behavior of the resilient (delay) time τ_d versus N. The delay time τ_d is conventionally defined by the relation $\sigma_{\max}(\tau_d) = 0.997$.

readily implemented in photonics using coupled waveguide arrays, as discussed, e.g., in Refs. [31,34]. The tight-binding band of the lattice is described by the dispersion relation $\omega(k) = 2\Delta \cos(k)$, where $-\pi \leqslant k < \pi$ is the Bloch wave number, whereas the discrete chain of N sites, when decoupled from the continuum, sustains N normal modes with energies $\omega_n = 2\kappa \cos[n\pi/(N+1)]$ and with excitation amplitudes (in the Wannier basis)

$$b_l^{(n)} = \sqrt{\frac{2}{N+1}} \sin\left(\frac{nl\pi}{N+1}\right), \tag{21}$$

where $l = 1, 2, \ldots, N$ is the Wannier site. The normal modes satisfy the orthonormality condition $(\mathbf{b}^{(n)}|\mathbf{b}^{(m)}) = \delta_{n,m}$. Indicating by $\hat{B}_n$ the destruction operator of particles at the n-Wannier site of the chain ($n = 1, 2, \ldots, N$) and by $\hat{A}_\alpha$ the destruction operator of particles at the αth site of the quantum wire ($\alpha = 0, \pm 1, \pm 2, \pm 3, \ldots$), in the nearest-neighbor tight-binding approximation the evolution equations for the

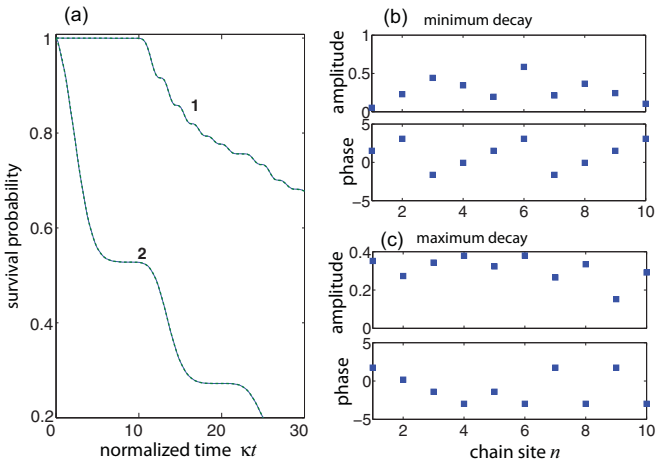

FIG. 3. (a) Numerically computed behavior of the survival probability $P(t)$ in the lattice model of Fig. 1(a) for $N = 10$, $\rho/\kappa = 1$, $\Delta/\kappa = 3$ and for two different initial coherent preparation $c_n(0)$ of the system, corresponding to delayed decay and accelerated decay. Curve 1 corresponds to the survival probability for the initial condition that maximizes $P(t)$ at $t = t_0 = 10/\kappa$ (delayed decay), whereas curve 2 corresponds to the survival probability for the initial condition that minimizes $P(t)$ at $t = t_0 = 10/\kappa$ (accelerated decay). Panels (b) and (c) show the amplitudes and phases of the initial coherent excitations $B_n(0)$ that minimize and maximize the decay in the Wannier basis of Fig. 1(a).

operators $\hat{B}_n$ and $\hat{A}_\alpha$ read

$$
\begin{aligned}
i\frac{d\hat{B}_n}{dt} &= \kappa(\hat{B}_{n+1} + \hat{B}_{n-1}) \quad (1 < n < N),\\
i\frac{d\hat{B}_1}{dt} &= \kappa\hat{B}_2 + \rho\hat{A}_0,\\
i\frac{d\hat{B}_N}{dt} &= \kappa\hat{B}_{N-1},\\
i\frac{d\hat{A}_\alpha}{dt} &= \Delta(\hat{A}_{\alpha+1} + \hat{A}_{\alpha-1}) + \rho\hat{B}_1\delta_{\alpha,0}.
\end{aligned}
\tag{22}
$$

The Friedrichs-Lee model (1) of quantum decay is readily obtained from Eqs. (22) after switching from Wannier to Bloch basis representation of operators. In fact, let us introduce the Bloch basis representation of operators via the relations

$$
\hat{c}_n = \sum_{l=1}^{N} b_l^{(n)}\hat{B}_l \quad (n = 1, 2, \ldots, N), \tag{23}
$$

$$
\hat{c}(k) = \frac{1}{\sqrt{2\pi}}\sum_{\alpha=-\infty}^{\infty}\hat{A}_\alpha \exp(ik\alpha). \tag{24}
$$

From Eqs. (22)–(24) it then readily follows that the evolution equations for the operators $\hat{c}_n$, $\hat{c}(k)$ in the Bloch basis are given by

$$
i\frac{d\hat{c}_n}{dt} = \omega_n\hat{c}_n(t) + \int_{-\pi}^{\pi} dk\, g_n(k)\hat{c}(k,t), \tag{25}
$$

$$
i\frac{\partial\hat{c}(k,t)}{\partial t} = \omega(k)\hat{c}(k,t) + \sum_{n=1}^{N} g_n^*(k)\hat{c}_n(t), \tag{26}
$$

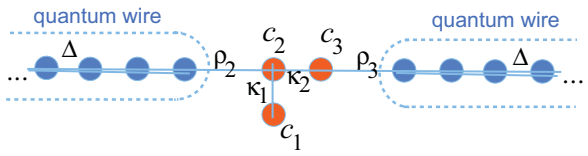

FIG. 4. Schematic of quantum mechanical decay of three Wannier sites (e.g., three quantum dots) attached to two leads (quantum wires). Anomalous decay from a third-order EP arises when conditions (32), (33) on intrahopping rates κ_1 and κ_2 are met.

where ω_n, $\omega(k)$, and $g_n(k)$ are given by Eqs. (17)–(19). Clearly, Eqs. (25) and (26) are the Heisenberg equations of motion for operators that one would obtain from the Friedrichs-Lee Hamiltonian (1).

The tight-binding lattice model of Fig. 1(a) is very helpful to provide a rather simple physical explanation of the resilient dynamics observed in the decay dynamics (Figs. 2 and 3), and the fact that the resilient time τ_d increases with the number N of discrete levels. In fact, let us assume that at initial time $t = 0$ the chain in Fig. 1(a) is excited in the site $n = N$, i.e., in the opposite edge of the chain coupled to the continuum. Clearly, the decay process into the continuum starts when the site $n = 1$, attached to the quantum wire, becomes excited. Since the excitation in the chain propagates by hopping at a finite speed $v \simeq 2\kappa$, for a time τ at least of the order $\tau \sim N/v \sim N/(2\kappa)$ the site $n = 1$ remains unexcited, and thus the decay into the continuum is delayed by such a time interval. This explains in a very simple (albeit qualitative) way why a resilient dynamics is observed in the multilevel quantum decay, and why the resilient time increases as the number N of levels is increased.

C. Anomalous decay at an exceptional point

In hydrodynamics flows, it has been known for a long time that non-normal dynamics is responsible for excess noise in the system and transient growth of perturbations, even by several orders of magnitude, despite the linear stability of the underlying flow [29,30]. A similar behavior occurs in multilevel quantum decay when the non-Hermitian matrix $\mathcal{H}$ is close to an EP. In fact, according to the general property (iii) stated in Sec. III A, the amplitude $F(t)$, that describes deviations from the exponential decay of the long-lived resonance of the system, undergoes a secular algebraic growth in time, indicating that—like in non-normal hydrodynamic flows—the spectral dominance of the long-lived resonance has little to do with the temporal behavior of the system. This property was earlier studied in the special case of two coalescing quantum resonances [31]; however, it was not related to non-normal dynamics of hydrodynamic flows. Here we suggest a rather simple model of quantum decay that gives rise to non-normal quantum decay at a third-order EP, thus showing a cubic behavior of $F(t)$ (rather than a quadratic one as in [31]). Also, in the proposed model we have two continuum of scattered states into which the discrete levels can decay. The system is schematically depicted in Fig. 4 and comprises three Wannier sites $|1\rangle$, $|2\rangle$, and $|3\rangle$, for example, three quantum dots, two of them attached to two semi-infinite tight-binding lattices

(i.e., two quantum wires) into which excitation decays. The quantum decay for this model can be emulated using photon transport in waveguide arrays, as discussed in [22,34]. Indicating by c_1, c_2, and c_3 the amplitude probabilities of excitation in the three Wannier sites $|1\rangle$, $|2\rangle$, and $|3\rangle$, respectively, after elimination of the excitation in the two quantum wires, the following effective non-Hermitian decay dynamics is obtained:

$$i\frac{d}{dt}\begin{pmatrix} c_1 \\ c_2 \\ c_3 \end{pmatrix} = \mathcal{H}\begin{pmatrix} c_1 \\ c_2 \\ c_3 \end{pmatrix}, \tag{27}$$

where

$$\mathcal{H} = \begin{pmatrix} 0 & \kappa_1 & 0 \\ \kappa_1 & -i\gamma_2 & \kappa_2 \\ 0 & \kappa_2 & -i\gamma_3 \end{pmatrix}. \tag{28}$$

In Eq. (28), κ_1 and κ_2 are the hopping amplitudes between sites $|1\rangle$, $|2\rangle$ and $|2\rangle$, $|3\rangle$, respectively (see Fig. 4), whereas γ_2 and γ_3 are the decay rates of sites $|2\rangle$ and $|3\rangle$ into the two quantum wires. They are given by

$$\gamma_2 \simeq \frac{\rho_2^2}{\Delta}, \quad \gamma_3 \simeq \frac{\rho_3^2}{\Delta}, \tag{29}$$

where ρ_2, ρ_3 are the hopping rates of Wannier states $|2\rangle$ and $|3\rangle$ to the attached quantum wire sites and $\Delta > \rho_{2,3}$ is the hopping rate between adjacent sites in the two quantum wires. The eigenvalues of the matrix (28) are the roots of the cubic equation

$$\lambda^3 + i(\gamma_2+\gamma_3)\lambda^2 - \left(\gamma_2\gamma_3 + \kappa_1^2 + \kappa_2^2\right)\lambda - i\gamma_3\kappa_1^2 = 0, \tag{30}$$

which are given by Cardano's formulas. From Cardano's relations, it can be readily shown that the three eigenvalues of $\mathcal{H}$ coalesce to the common value

$$\lambda = -i(\gamma_2+\gamma_3)/3 \tag{31}$$

when the intracoupling constants κ_1 and κ_2 satisfy the conditions

$$\kappa_1 = \sqrt{\frac{(\gamma_2+\gamma_3)^3}{27\gamma_3}}, \tag{32}$$

$$\kappa_2 = \sqrt{\frac{(\gamma_2+\gamma_3)^2(8\gamma_3-\gamma_2) - 27\gamma_2\gamma_3^2}{27\gamma_3}}. \tag{33}$$

The corresponding eigenvectors also coalesce to the common vector

$$\mathbf{v}_1 \propto \begin{pmatrix} 3\kappa_1 \\ -i(\gamma_2+\gamma_3) \\ \frac{3\kappa_2(\gamma_2+\gamma_3)}{\gamma_2-2\gamma_3} \end{pmatrix}. \tag{34}$$

Therefore, as the hopping amplitudes κ_1 and κ_2 are tuned to satisfy Eqs. (32) and (33), a third-order EP is found: the matrix $\mathcal{H}$, besides being non-normal, becomes nondiagonalizable at such values of hopping amplitudes. This means that, for a generic initial state preparation of the system, the survival probability shows an exponential-algebraic decay, rather than a purely exponential decay with the decay rate given by the unique eigenvalue (31) of $\mathcal{H}$.

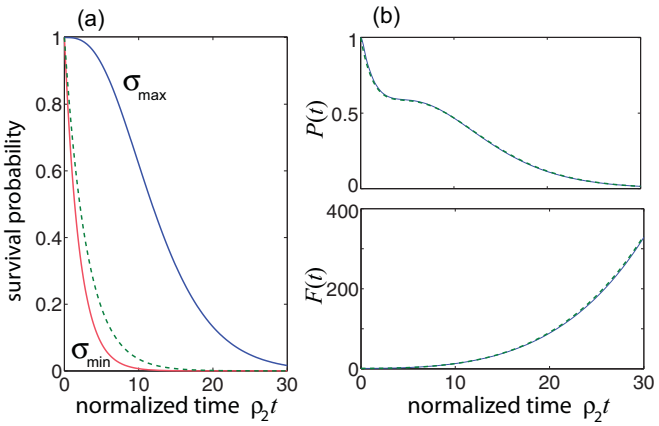

FIG. 5. (a) Numerically computed behaviors of the upper ($\sigma_{\max}$) and lower ($\sigma_{\min}$) boundaries of the survival probability $P(t)$ versus normalized time for the tight-binding lattice model of Fig. 4. Parameter values are given in the text. The dashed curve shows the exponential decay behavior of the coalescing resonance modes at the EP. (b) Survival probability $P(t)$ versus normalized time (upper plot), and corresponding envelope $F(t)$ (lower plot), corresponding to the initial excitation of the three Wannier states in the eigenvector of the adjoint matrix $\mathcal{H}^\dagger$. Solid and dashed curves, almost overlapped, refer to numerical results obtained for the full model and for the reduced matrix (28) (Markovian approximation).

As an example, Fig. 5 shows numerical results of quantum-mechanical decay in the structure of Fig. 4 for parameter values $\rho_3/\rho_2 = 1$, $\Delta/\rho_2 = 4$ and for the intercoupling hopping amplitudes κ_1 and κ_2 tuned to satisfy Eqs. (32) and (33), i.e., $\kappa_1/\rho_2 \simeq 0.1361$ and $\kappa_2/\rho_2 \simeq 0.0481$. Figure 5(a) depicts the behavior of upper ($\sigma_{\max}$) and lower ($\sigma_{\min}$) boundaries of the survival probability $P(t)$, along with the exponential decay of the coalescing resonances of the system. The behavior of $P(t)$, corresponding to the initial excitation of the three quantum dots in the eigenvector of the adjoint matrix $\mathcal{H}$, is shown in Fig. 4(b). Deviation from exponential decay, corresponding to an algebraic (cubic) increase of $F(t)$, is clearly observed.

IV. MULTIPARTICLE QUANTUM DECAY

The previous analysis has been focused to the decay dynamics of a single particle. However, in many particle systems the decay dynamics is known to be largely influenced by contact interactions and particle statistics [21,22]. For example, for noninteracting particles the long-time algebraic decay law of indistinguishable particles differs from the single-particle decay law and depends on the statistics of the particles, fermions showing a faster decay than bosons. A recent experiment [22] that used polarization-entangled photon states to emulate different particle statistics clearly showed that quantum decay is affected by particle statistics. Thus a main question arises: in the case of multilevel and multiparticle quantum decay, how does particle statistics affect non-normal decay dynamics? An important and rather simple result, that is proved below, is the following one: all anomalous decay features arising from non-normal dynamics in the single particle case, such as resilient

(delayed) decay, accelerated decay, and exponential-power-law decay at an EP, are fully washed out when considering the decay of $G = N$ noninteracting fermionic particles. In fact, let us consider the N-level Friedrichs-Lee Hamiltonian (1), and let us assume that $G = N$ spineless particles with fermionic statistics are initially occupying the N discrete levels. Owing to the Pauli exclusion principle, each level can be empty or occupied by one particle solely. The survival probability $P^{(\mathrm{ferm})}(t)$ that at time t none of the G particles has decayed into the continuum is given by [22]

$$P^{(\mathrm{ferm})}(t) = |\det(\mathcal{A})|^2, \tag{35}$$

where $\mathcal{A} = \exp(-i\mathcal{H}t)$ and $\mathcal{H}$ is the non-Hermitian matrix given by Eq. (8). Using the property that $\det(\exp(-i\mathcal{H}t)) = \exp(-it\,\mathrm{Tr}(\mathcal{H}))$, from Eq. (8) one obtains

$$P^{(\mathrm{ferm})}(t) = \exp(-\gamma t), \tag{36}$$

where we have set $\gamma = 2\sum_{n=1}^{N}\Delta_{n,n}$. Equation (36) shows that in the Markovian approximation the survival probability is exactly given by an exponential curve with effective decay rate γ, i.e., anomalous decay features, observed for the single-particle decay and arising from the non-normal nature of $\mathcal{H}$, are fully canceled. Note that this result holds only for fermionic particles and provided that the number G of particles equals the number N of discrete states.

V. CONCLUSION

Quantum mechanics predicts that, beyond the Weisskopf-Wigner approximation, the decay of a metastable state coupled to a continuum deviates from an exponential law at both short and long time scales. Such deviations, in particular the lower-than-exponential decay at short times, have attracted great interest, since frequent observations of the decay state could in principle slow down or even suppress the decay process (quantum Zeno effect). The decay of several metastable states into a continuum shows a richer dynamical scenario that arises from interference of decaying resonances. For example, destructive interference of different decay channels can lead to fractional (limited) decay owing to the existence of bound states in the continuum (dark states). In this work we have theoretically studied on a general basis anomalous decay behaviors in multilevel quantum systems under the Markovian approximation. Our results show that the variety of behaviors observed in multilevel quantum decay originate from the non-normal nature of the effective non-Hermitian Hamiltonian that describes quantum decay, revealing strong similarities between multilevel quantum decay and non-normal dynamics observed in hydrodynamic flows. Major signatures of non-normal dynamics include resilient dynamics and delayed decay, accelerated decay, and exponential-power-law decay at an exceptional point. Such signatures have been exemplified by suggesting simple tight-binding lattice realizations of multilevel quantum decay, which could be emulated in integrated photonic experiments. Finally, we have shown quite remarkably that non-normal dynamical features of multilevel quantum decay are fully washed out and exponential decay is restored when considering the decay dynamics of noninteracting spinless particles with fermionic statistics.

APPENDIX A: GENERAL PROPERTIES OF NON-NORMAL QUANTUM DECAY

In this appendix we prove the general properties of non-normal quantum decay given in Sec. III A. For a system prepared in a coherent superposition of amplitudes $\mathbf{c}(0) \equiv (c_1(0), c_2(0), \ldots, c_N(0))^T$, in the Markovian approximation [Eq. (7)] the amplitudes $\mathbf{c}(t)$ at a subsequent time t are given by

$$\mathbf{c}(t) = \mathcal{A}\mathbf{c}(0), \tag{A1}$$

where the evolution operator $\mathcal{A}$ is given by

$$\mathcal{A} = \exp(-i\mathcal{H}t). \tag{A2}$$

The survival probability $P(t)$ at time t is thus given by

$$P(t) = (\mathbf{c}(t)|\mathbf{c}(t)) = (\mathcal{A}\mathbf{c}(0)|\mathcal{A}\mathbf{c}(0)) = (\mathbf{c}(0)|\mathcal{A}^\dagger\mathcal{A}\mathbf{c}(0)), \tag{A3}$$

where $(\mathbf{f}|\mathbf{g}) \equiv \sum_n g_n^* f_n$ denotes the usual l^2 scalar product. From Eq. (A3) it then follows that

$$\sigma_{\min}(t) \leqslant P(t) \leqslant \sigma_{\max}(t), \tag{A4}$$

where

$$\sigma_{\max} \equiv \max_{(\mathbf{c}(0)|\mathbf{c}(0))=1} (\mathbf{c}(0)|\mathcal{A}^\dagger\mathcal{A}\mathbf{c}(0)), \tag{A5}$$

$$\sigma_{\min} \equiv \min_{(\mathbf{c}(0)|\mathbf{c}(0))=1} (\mathbf{c}(0)|\mathcal{A}^\dagger\mathcal{A}\mathbf{c}(0)). \tag{A6}$$

Note that $\sigma_{\max}(t)$ is the 2-norm of the self-adjoint matrix $\mathcal{A}^\dagger\mathcal{A}$. Since $\mathcal{A}^\dagger\mathcal{A}$ is a self-adjoint and positive-definite matrix, $\sigma_{\max}(t)$ and $\sigma_{\min}(t)$ correspond to the largest and the smallest eigenvalues of $\mathcal{A}^\dagger\mathcal{A}$, respectively. Moreover, the equalities in Eq. (A4) are attained when $\mathbf{c}(0)$ is equal to the eigenvector of $\mathcal{A}^\dagger\mathcal{A}$ with eigenvalue $\sigma_{\max}$ and $\sigma_{\min}$, respectively. This proves property (i) given in Sec. III A.

If $\mathcal{H}$ is a normal operator, i.e., if $\mathcal{H}$ commutes with $\mathcal{H}^\dagger$, one has

$$\mathcal{A}^\dagger\mathcal{A} = \exp(i\mathcal{H}^\dagger t)\exp(-i\mathcal{H}t) = \exp(\mathcal{L}t), \tag{A7}$$

where $\mathcal{L} =\equiv i(\mathcal{H}^\dagger - \mathcal{H})$. Note that $\mathcal{L}$ is a Hermitian operator and its eigenvalues are real and positive. The largest eigenvalue $\sigma_{\max}$ of $\exp(\mathcal{L}t)$ is clearly given by $\exp(-t/\tau)$, where $1/\tau = -2\,\mathrm{Im}(\lambda_1)$, and it is assumed when $\mathbf{c}(0)$ is the eigenvector of $\mathcal{H}$ with eigenvalue λ_1, i.e., when the system is prepared in the long-lived resonance mode. Likewise, the smallest eigenvalue of $\exp(\mathcal{L}t)$ is given by $\exp(-2t|\mathrm{Im}(\lambda_N)|)$. This proves property (ii) given in Sec. III A.

Finally, let us assume that the non-Hermitian matrix $\mathcal{H}$ is defective and its eigenvalue λ_1 is an EP of order h. For the sake of simplicity, let us assume $h = N$, i.e., let us assume that all eigenvalues and corresponding eigenvectors of $\mathcal{H}$ coalesce; however, the results given below can be extended to the more general case $h < N$. Let us indicate by $\mathbf{v}_1$ the eigenvector of $\mathcal{H}$ with eigenvalue λ_1, and by $\mathbf{u}_2, \mathbf{u}_3, \ldots, \mathbf{u}_N$ the chain of associated (generalized) eigenvectors, defined by the chain

(see also Appendix B)

$$\begin{aligned}(\mathcal{H}-\lambda_1)\mathbf{v}_1 &= 0,\\ (\mathcal{H}-\lambda_1)\mathbf{u}_2 &= i\mathbf{v}_1,\\ &\cdots\ \cdots\ \cdots,\\ (\mathcal{H}-\lambda_1)\mathbf{u}_N &= i\mathbf{u}_{N-1}.\end{aligned} \tag{A8}$$

A set of N linearly independent solutions to Eq. (7) is given by

$$\begin{aligned}\mathbf{c}_1(t) &= \frac{\exp(-i\lambda_1 t)}{\sqrt{(\mathbf{v}_1|\mathbf{v}_1)}}\mathbf{v}_1,\\ \mathbf{c}_2(t) &= \frac{\exp(-i\lambda_1 t)}{\sqrt{(\mathbf{u}_2|\mathbf{u}_2)}}(\mathbf{u}_2+t\mathbf{v}_1),\\ \mathbf{c}_3(t) &= \frac{\exp(-i\lambda_1 t)}{\sqrt{(\mathbf{u}_3|\mathbf{u}_3)}}\left(\mathbf{u}_3+t\mathbf{u}_2+\frac{t^2}{2!}\mathbf{v}_1\right),\\ &\cdots\ \cdots\ \cdots,\\ \mathbf{c}_N(t) &= \frac{\exp(-i\lambda_1 t)}{\sqrt{(\mathbf{u}_N|\mathbf{u}_N)}}\left(\mathbf{u}_N+t\mathbf{u}_{N-1}+\cdots+\frac{t^{N-1}}{(N-1)!}\mathbf{v}_1\right).\end{aligned} \tag{A9}$$

Clearly, in the asymptotic limit $t\to\infty$ the dominant (long-lived) contribution to $\mathbf{c}(t)$, for a given initial condition $\mathbf{c}(0)$, is provided by the term $\mathbf{c}_N(t)$, which shows a power-law exponential decay $\sim t^{N-1}\exp(-i\lambda_1 t)$. Therefore, in this limit the largest value $\sigma_{\max}(t)$ is attained when the system is initially prepared in the state $\mathbf{c}(0)=\mathbf{u}_N/\sqrt{(\mathbf{u}_N|\mathbf{u}_N)}$, so that $\mathbf{c}(t)=\mathbf{c}_N(t)$ and

$$\sigma_{\max}(t)\simeq\frac{(\mathbf{v}_1|\mathbf{v}_1)t^{2(N-1)}}{[(N-1)!]^2(\mathbf{u}_N|\mathbf{u}_N)}\exp(-t/\tau) \tag{A10}$$

as $t\to\infty$. This proves property (iii) given in Sec. III A.

APPENDIX B: EXCEPTIONAL POINTS, JORDAN FORM, AND ASSOCIATED EIGENVECTORS

Let $\mathcal{H}=\mathcal{H}(\mathbf{R})$ be an $N\times N$ matrix, which depends on some real parameters described by $\mathbf{R}$, and let us indicate by $\lambda_1(\mathbf{R}),\lambda_2(\mathbf{R}),\ldots,\lambda_N(\mathbf{R})$ the N eigenvalues of $\mathcal{H}$, which are generally complex since $\mathcal{H}$ is not a Hermitian matrix. A remarkable property of non-Hermitian matrices compared with Hermitian ones is that, as $\mathbf{R}$ is varied, eigenvalues and eigenstates of $\mathcal{H}$ can show bifurcation and accompanying nonanalyticity. A point $\mathbf{R}=\mathbf{R}_0$ in parameter space where this kind of bifurcation takes place is called an exceptional point (EP) [32,33]. At an EP, a non-Hermitian degeneracy occurs, i.e., $h\geqslant 2$ eigenvalues *and* corresponding eigenvectors of $\mathcal{H}(\mathbf{R}=\mathbf{R}_0)$ coalesce. h is referred to as the *order* of EP. Since at an EP there is at least one eigenvalue with a geometric multiplicity (i.e., dimension of its eigenspace) which is strictly less than its algebraic multiplicity (so-called *defective* eigenvalue), the eigenvectors of $\mathcal{H}$ at $\mathbf{R}=\mathbf{R}_0$ do not form a complete basis and the matrix $\mathcal{H}$ cannot be diagonalized. However, $\mathcal{H}$ can always be reduced to Jordan normal form [35,36]. To overcome the deficiency of eigenvectors of a non-Hermitian matrix at the EP, one should introduce the so-called *generalized* (or associated) eigenvectors, which can in turn be used to find the Jordan form of the matrix $\mathcal{H}$ [35,36]. At an EP of order h, the eigenvalues $\lambda_1(\mathbf{R}_0),\lambda_2(\mathbf{R}_0),\ldots,\lambda_h(\mathbf{R}_0)$ take the same value λ_1 with the same eigenvector $\mathbf{v}_1$,

$$(\mathcal{H}-\lambda_1)\mathbf{v}_1=0, \tag{B1}$$

while the other eigenvalues $\lambda_{h+1}(\mathbf{R}_0),\lambda_{h+2}(\mathbf{R}_0),\ldots,\lambda_N(\mathbf{R}_0)$ are distinct or not defective, i.e.,

$$(\mathcal{H}-\lambda_n)\mathbf{v}_n=0 \tag{B2}$$

$(n=h+1,h+2,\ldots,N)$, with $\{\mathbf{v}_n\}_{n>h}$ linearly independent. The chain of associated eigenvectors $\mathbf{u}_2,\mathbf{u}_3,\ldots,\mathbf{u}_h$ of $\mathbf{H}$, corresponding to the defective eigenvalue λ_1, is defined by Eq. (A8). Note that, for each $n=2,3,\ldots,h$, one has $(\mathcal{H}-\lambda_1)^n\mathbf{u}_n=0$ but $(\mathcal{H}-\lambda_1)^{n-1}\mathbf{u}_n\neq 0$. The vectors $\mathbf{v}_1,\mathbf{u}_2,\ldots,\mathbf{u}_h,\mathbf{v}_{h+1},\ldots,\mathbf{v}_N$ are linearly independent and thus form a complete basis of Hilbert space. By the similarity transformation

$$\mathcal{H}=\mathcal{C}\mathcal{J}\mathcal{C}^{-1}, \tag{B3}$$

the matrix $\mathcal{H}$ can be reduced to the Jordan normal form

$$\mathcal{J}=\left(\begin{array}{c|c}\mathcal{A}&0\\\hline 0&\mathcal{B}\end{array}\right), \tag{B4}$$

where the $h\times h$ and $(N-h)\times(N-h)$ matrices $\mathcal{A}$ and $\mathcal{B}$ are given by

$$\mathcal{A}=\begin{pmatrix}\lambda_1&1&0&0&\ldots&0\\0&\lambda_1&1&0&\ldots&0\\\ldots&\ldots&\ldots&\ldots&\ldots&\ldots\\0&0&\ldots&0&\lambda_1&1\\0&0&\ldots&0&0&\lambda_1\end{pmatrix}, \tag{B5}$$

$$\mathcal{B}=\begin{pmatrix}\lambda_{h+1}&0&0&0&\ldots&0\\0&\lambda_{h+2}&0&0&\ldots&0\\\ldots&\ldots&\ldots&\ldots&\ldots&\ldots\\0&0&\ldots&0&\lambda_{N-1}&0\\0&0&\ldots&0&0&\lambda_N\end{pmatrix}. \tag{B6}$$

The matrix $\mathcal{C}$ is constructed from the eigenvectors and the chain of associated eigenvectors of $\mathcal{H}$ [35,36]. Also, the matrix $\mathcal{C}$ can be used to find a set of linearly independent solutions to the ordinary differential system of equations $id\mathbf{v}/dt=\mathcal{H}\mathbf{v}$ [35,36]. In particular, for the limiting case $h=N$ the set of N linearly independent solutions of the linear system are given by Eqs. (A9).

As a final remark, we note that non-normality of the matrix $\mathcal{H}$ is a necessary (but not sufficient) condition for $\mathcal{H}$ to show an EP. In fact, the matrix $\mathcal{H}$ is normal if and only if it is unitarily diagonalizable: hence a normal matrix cannot show EPs. However, the condition of nondiagonalizability of $\mathcal{H}$, i.e., the appearance of an EP, is a much more stringent requirement than non-normality. Indeed, a non-normal matrix can be diagonalizable, while EPs of a non-normal matrix arise for some special values of the control parameters (see the example of Sec. III C).

[1] G. Gamow, Z. Phys. **51**, 204 (1928).
[2] V. F. Weisskopf and E. Wigner, Z. Phys. **63**, 54 (1930).
[3] R. G. Winter, Phys. Rev. **123**, 1503 (1961).
[4] L. Fonda, G. C. Ghirardi, and A. Rimini, Rep. Prog. Phys. **41**, 587 (1978).
[5] P. L. Knight, M. A. Lauder, and B. J. Dalton, Phys. Rep. **190**, 1 (1990).
[6] H. Nakazato, M. Namiki, and S. Pascazio, Int. J. Mod. Phys. B **10**, 247 (1996).
[7] P. Facchi and S. Pascazio, *La Regola d'oro di Fermi* (Bibliopolis, Napoli, 1999).
[8] J. Martorell, J. G. Muga, and W. L. Sprung, Lect. Notes Phys. **789**, 239 (2009).
[9] E. J. Hellund, Phys. Rev. **89**, 919 (1953).
[10] L. A. Khalfin, Sov. Phys. JETP **6**, 1053 (1958).
[11] J. G. Muga, G. W. Wei, and R. F. Snider, Europhys. Lett. **35**, 247 (1996); J. Martorell, J. G. Muga, and D. W. L. Sprung, Phys. Rev. A **77**, 042719 (2008).
[12] S. Garmon, T. Petrosky, L. Simine, and D. Segal, Fortschr. Phys. **61**, 261 (2013).
[13] S. R. Wilkinson, C. F. Bharucha, M. C. Fischer, K. W. Madison, P. R. Morrow, Q. Niu, B. Sundaram, and M. G. Raizen, Nature (London) **387**, 575 (1997).
[14] C. Rothe, S. I. Hintschich, and A. P. Monkman, Phys. Rev. Lett. **96**, 163601 (2006).
[15] C. B. Chiu, B. Misra, and E. C. G. Sudarshan, Phys. Rev. D **16**, 520 (1977).
[16] A. G. Kofman and G. Kurizki, Nature (London) **405**, 546 (2000); Phys. Rev. Lett. **87**, 270405 (2001).
[17] M. C. Fischer, B. Gutierrez-Medina, and M. G. Raizen, Phys. Rev. Lett. **87**, 040402 (2001).
[18] P. Facchi, H. Nakazato, and S. Pascazio, Phys. Rev. Lett. **86**, 2699 (2001).
[19] J. M. Raimond, P. Facchi, B. Peaudecerf, S. Pascazio, C. Sayrin, I. Dotsenko, S. Gleyzes, M. Brune, and S. Haroche, Phys. Rev. A **86**, 032120 (2012).
[20] M. A. Porras, A. Luis, I. Gonzalo, and A. S. Sanz, Phys. Rev. A **84**, 052109 (2011).
[21] A. del Campo, F. Delgado, G. Garcia-Calderon, J. G. Muga, and M. G. Raizen, Phys. Rev. A **74**, 013605 (2006); A. U. J. Lode, A. I. Streltsov, O. E. Alon, H.-D. Meyer, and L. S. Cederbaum, J. Phys. B **42**, 044018 (2009); T. Taniguchi and S. I. Sawada, Phys. Rev. E **83**, 026208 (2011); A. del Campo, Phys. Rev. A **84**, 012113 (2011); G. Garcia-Calderon and L. G. Mendoza-Luna, *ibid.* **84**, 032106 (2011); M. Rontani, Phys. Rev. Lett. **108**, 115302 (2012); M. Pons, D. Sokolovski, and A. del Campo, Phys. Rev. A **85**, 022107 (2012); A. Del Campo, New J. Phys. **18**, 015014 (2016).
[22] S. Longhi and G. Della Valle, Phys. Rev. A **86**, 012112 (2012); A. Crespi, L. Sansoni, G. Della Valle, A. Ciamei, R. Ramponi, F. Sciarrino, P. Mataloni, S. Longhi, and R. Osellame, Phys. Rev. Lett. **114**, 090201 (2015).
[23] M. Miyamoto, Phys. Rev. A **70**, 032108 (2004); J. Mater. Phys. **47**, 082103 (2006).
[24] H. Friedrich and D. Wintgen, Phys. Rev. A **32**, 3231 (1985); G. Sudarshan, in *Field Theory, Quantization and Statistical Physics*, edited by E. Tirapegui (Reidel, Dordrecht, Holland, 1988), pp. 237–245; M. Miyamoto, Phys. Rev. A **72**, 063405 (2005).
[25] H. Nakamura, N. Hatano, S. Garmon, and T. Petrosky, Phys. Rev. Lett. **99**, 210404 (2007); S. Longhi, Eur. J. Phys. B **57**, 45 (2007); J. Mod. Opt. **56**, 729 (2009); S. Garmon, H. Nakamura, N. Hatano, and T. Petrosky, Phys. Rev. B **80**, 115318 (2009); F. Dreisow, A. Szameit, M. Heinrich, R. Keil, S. Nolte, A. Tünnermann, and S. Longhi, Opt. Lett. **34**, 2405 (2009).
[26] I. Antoniou, E. Karpov, G. Pronko, and E. Yarevsky, Int. J. Theor. Phys. **42**, 2403 (2003).
[27] E. Frishman and M. Shapiro, Phys. Rev. Lett. **87**, 253001 (2001); Phys. Rev. A **68**, 032717 (2003).
[28] H. Cartarius and N. Moiseyev, Phys. Rev. A **84**, 013419 (2011); B. Dietz, T. Friedrich, J. Metz, M. Miski-Oglu, A. Richter, F. Schäfer, and C. A. Stafford, Phys. Rev. E **75**, 027201 (2007); S. Garmon and G. Ordonez, J. Math. Phys. **58**, 062101 (2017).
[29] S. C. Reddy and D. S. Henningson, J. Fluid Mech. **252**, 209 (1993); L. N. Trefethen, A. E. Trefethen, S. C. Reddy, and T. A. Driscoll, Science **261**, 578 (1993); S. C. Reddy, P. J. Schmid, and D. S. Henningson, SIAM J. Appl. Math. **53**, 15 (1993); L. N. Trefethen, SIAM Rev. **39**, 383 (1997).
[30] B. F. Farrell and P. J. Ioannou, Phys. Fluids A **5**, 2600 (1993); Phys. Rev. Lett. **72**, 1188 (1994); J. Atmos. Sci. **53**, 2025 (1996).
[31] S. Longhi, Laser Photon. Rev. **3**, 243 (2009).
[32] T. Kato, *Perturbation Theory for Linear Operators* (Springer, Berlin, 1976), Vol. 132.
[33] W. D. Heiss, J. Phys. A **37**, 2455 (2004).
[34] F. Dreisow, A. Szameit, M. Heinrich, T. Pertsch, S. Nolte, A. Tünnermann, and S. Longhi, Phys. Rev. Lett. **101**, 143602 (2008); P. Biagioni, G. Della Valle, M. Ornigotti, M. Finazzi, L. Duó, P. Laporta, and S. Longhi, Opt. Express **16**, 3762 (2008); S. Longhi, Phys. Rev. Lett. **97**, 110402 (2006).
[35] F. R. Gantmacher, *Matrix Theory* (Chelsea, New York, 1959).
[36] R. A. Horn and C. R. Johnson, *Matrix Analysis*, 2nd ed. (Cambridge University Press, Cambridge, UK, 2012).